Journal of Applied Polymer Science

Thermal, mechanical, and structural properties of ZnO/polyethylene membranes made by thermally induced phase separation method

Yoones Jafarzadeh,[1,2] Reza Yegani[1,2]

[1]Faculty of Chemical Engineering, Sahand University of Technology, Sahand New Town, Tabriz 51335/1996, Iran
[2]Membrane Technology Research Center, Sahand University of Technology, Sahand New Town, Tabriz 51335/1996, Iran
Correspondence to: R. Yegani (E-mail: ryegani@sut.ac.ir)

ABSTRACT: In this study, ZnO/polyethylene membranes were fabricated via thermally induced phase separation method. A set of tests including FE-SEM, EDX, XRD, DSC, TGA, DMA, mechanical test, and pure water flux (PWF) for characterization of membranes were carried out. The results of EDX, XRD, and TGA analyses confirmed the presence of ZnO nanoparticles in the polymer matrix. The results of DSC analysis revealed that the melting point as well as the crystallinity of the membranes increased slightly with increasing ZnO content. However, glass transition temperature of the membranes was not affected by presence of the particles. Addition of nanoparticles also increased storage modulus, loss modulus. and tensile at break of the membranes due to the stiffness improvement effect of inorganic ZnO. Finally, it was observed that incorporation of the nanoparticles improved PWF of the membranes, whereas humic acid rejection decreased due to the increase in mean pore radius of membranes. © 2015 Wiley Periodicals, Inc. J. Appl. Polym. Sci. **2015**, *132*, 42338.

KEYWORDS: membranes; polyolefins; thermal properties

Received 4 February 2015; accepted 8 April 2015
DOI: 10.1002/app.42338

INTRODUCTION

Due to the hydrophobic characteristics, most of the polymeric membranes show low water permeability and are susceptible to fouling. Therefore, many efforts have been devoted to reduce fouling in hydrophobic polymer membranes. Generally, three different approaches have been described in the literature to increase membranes' hydrophilicity including premodification of polymers before membrane synthesis,[1] incorporation of inorganic and/or organic additives during membrane preparation,[2–4] and postmodification of membrane surface via different methods such as plasma surface treatment and dip-coating.[5,6] Among them, incorporation of inorganic nanoparticles into membranes has attracted most attentions because of the simplicity and the lack of additional steps in the membrane preparation steps.[7]

Recently, nanoparticles have been widely used in the manufacturing of membranes because of their unique physicochemical properties. It has been shown that antifouling properties of polymer membranes can be improved by using of nanoparticles.[4,8] In this method, nanoparticles with appropriate properties are dispersed through the membrane bulk and, therefore, internal pores of the membrane could also be impacted. These particles also improve the mechanical strength of the polymeric membranes, which is a requirement for sever service conditions in fouled membranes.

Polyethylene (PE) membranes are widely used in different membrane processes such as membrane distillation, membrane extraction, blood oxygenators, biosensors, and water treatment due to its excellent mechanical strength, chemical resistance, and thermal stability while being a low-cost material compared to other commercial polymers.[9–11] PE membranes, however, suffer from nonwettability and poor biocompatibility due to the nonpolar nature of PE chains and, therefore, limits their application in separation of aqueous solutions, biomedical fields, and water treatment.[10,12,13] In other words, due to the nonpolar backbone of PE polymer, the fabricated membranes are very susceptible to fouling because of their inherent hydrophobicity.[14,15] Therefore, incorporation of hydrophilic nanoparticles seems to be an effective manner to increase antifouling properties of PE membranes.

Nanoparticles that have been widely used in polymer-inorganic membranes include ZrO_2,[16] TiO_2,[17] Al_2O_3,[18] SiO_2,[19] and ZnO.[3,4] ZnO is a multifunctional semiconductor which due to its desirable properties such as hydrophilicity, antifouling abilities, photocatalytic activities, stability, and availability has been recently used in inorganic particle-embedded polymer membranes.[4,20,21] Several studies have investigated the incorporation of ZnO nanoparticles into different polymers including polyethersulfone (PES),[4,21] polyvinilidenfluoride (PVDF),[3] and

polysulfone (PSf).[20] In our previous work,[22] we successfully fabricated ZnO-embedded high-density polyethylene (HDPE) membranes via thermally induced phase separation (TIPS) method and compared their fouling behavior and characteristics with neat HDPE membrane. Obtained results were promising and clearly showed that incorporation of ZnO nanoparticles could considerably enhance the fouling behavior of PE membrane. However, no deep discussion was performed on the structural aspects of nanocomposite membranes. In this work, we are going to study the impact of ZnO nanoparticles on the properties of fabricated membranes using a set of experiments such as field-emission scanning electron microscopy (FE-SEM), energy-dispersive X-ray (EDX) spectroscopy, X-ray diffraction (XRD), differential scanning calorimetry (DSC), dynamic mechanical analyzer (DMA), thermogravimetric analysis (TGA), mechanical strength, and pure water flux (PWF). Moreover, the performance of membranes was studied by filtration of humic acid solution as an important water contaminant.

EXPERIMENTAL

Materials

The commercial grade of HDPE (with average molecular weight of *ca* 119,500 g/mol) was provided by Amirkabir Petrochemical Company and used as polymer. ZnO nanoparticles (particle size <100 nm) were purchased from Sigma Aldrich. Mineral oil (MO) as diluent and acetone as extractant were purchased from Acros Organics and Merck, respectively. Humic acid was purchased from Merck. All materials were used without further purification.

Preparation of Membranes

TIPS method was applied to prepare neat and ZnO-embedded membranes. Different amounts of ZnO nanoparticles (0.25, 0.50, 0.75, and 1.00 g) were dispersed into 79.75, 79.50, 79.25, and 79.00 g of MO, respectively, using sonication by probe system (Sonopuls HD 3200, Bandelin) for 15 min. Then 20 g of HDPE was gradually added to the diluent–nanoparticle suspension and melt-blended at 160°C for 90 min in a sealed glass vessel kept in a silicon oil bath. The solution was then allowed to degas for 30 min and cast on a preheated glass sheet using a doctor blade. The plate was immediately quenched in the water bath (27°C ± 3) to induce phase separation. The membrane was then immersed in acetone for 24 h to extract its diluent. Finally, it was dried at room temperature to remove acetone. The results of DSC analysis (not shown here) revealed that the acetone in the membranes was removed during drying at room temperature. In the case of neat membrane, mineral oil and HDPE was melt-blended at 160°C for 90 min in a sealed glass vessel kept in a silicon oil bath. Other procedures were the same to the ZnO-embedded membranes preparation.

Membrane Characterization

SEM and EDX. The morphology of the membranes was characterized by FE-SEM (MIRA3 FEG-SEM, Tescan). Cross-section samples were prepared by fracturing the membranes in liquid nitrogen. All samples were coated with gold by sputtering before observation. The existence of ZnO nanoparticles in the membranes were analyzed by EDX (MIRA3 FEG-SEM, Tescan).

XRD Analysis. XRD study of the membranes was conducted using a diffractometer (D8 Advance, Bruker) equipped with monochromatic Cu-K_α radiation ($\lambda = 0.154$ nm) under a voltage of 40 kV and a current of 40 mA. All samples were analyzed in continuous scan mode with the 2θ ranging from 10° to 80°.

DSC Analysis. The melting and crystallization behavior of composite membranes were studied by DSC (DSC 4000, PerkinElmer) in nitrogen atmosphere. The samples were heated from 25 to 200°C at 10°C/min and held at 200°C for 5 min, followed by cooling back to 25°C at 10°C/min and held for another 5 min. Finally, they were reheated to 200°C at the same rate. Melting point (T_m) and crystallization point (T_c) of the samples were taken from the peaks of second heating and first cooling, respectively. The percentage of crystallinity (χ_c) of the samples were calculated as follows:

$$\chi_c = \left[\frac{\Delta H_m}{\Delta H_m^0 (1 - w_{ZnO})}\right] \times 100 \quad (1)$$

where, w_{ZnO} is the mass composition of nanoparticles in the samples, ΔH_m is the enthalpy of melting of the samples, and ΔH_m^0 is the extrapolated value of enthalpy corresponding to 100% crystalline PE which was obtained from literature as $\Delta H_m^0 = 293$ *J/g*.[23] It should be noted that the value of w_{ZnO} in eq. (1) is the composition of zinc oxide nanoparticle in the final membrane and not the initial casting solution.

Thermogravimetric Analysis. The quality of dispersion of ZnO nanoparticles in the fabricated membranes was investigated using a thermogravimetric analyzer (Pyris Diamond TG/DTA, PerkinElmer) at a heating rate of 10°C/min from ambient temperature to 600°C under nitrogen atmosphere.

Mechanical Properties. Dynamic mechanical properties of the nanocomposite membranes were measured with a Perkin-Elmer Diamond DMA. The tests were conducted by temperature sweep mode at a frequency of 1 Hz and temperature range of −100 to 50°C. Information on storage module (E'), loss module (E''), and glass transition temperature were collected for each sample.

Tensile strength and elongation at break of membranes were determined using a tensile testing machine (STM-5, Santam) at an extension rate of 50 mm/min. The samples were cut in 80 mm in length and 15 mm in width. The thickness of samples varied between 410 and 430 μm because of shrinkage of membranes during extraction of mineral oil in the preparation step. Each membrane was tested at least 3 times and averaged values were reported.

Pure Water Flux. PWF of the membranes was determined using an in-house-fabricated dead-end filtration system having 5 cm^2 of membrane area. To minimize the compaction effects, the prewetted membranes were compacted for 30 min at 2 bar. Then the pressure was reduced to 1.4 bar and after reaching steady state, water flux was calculated using the following equation:

$$J = \frac{M}{A.t} \quad (2)$$

where J is the PWF, M is the collected mass of water (kg), A is the membrane area (m^2), and t is the time (h). Relative PWF, J_r, was then calculated according to the following equation:

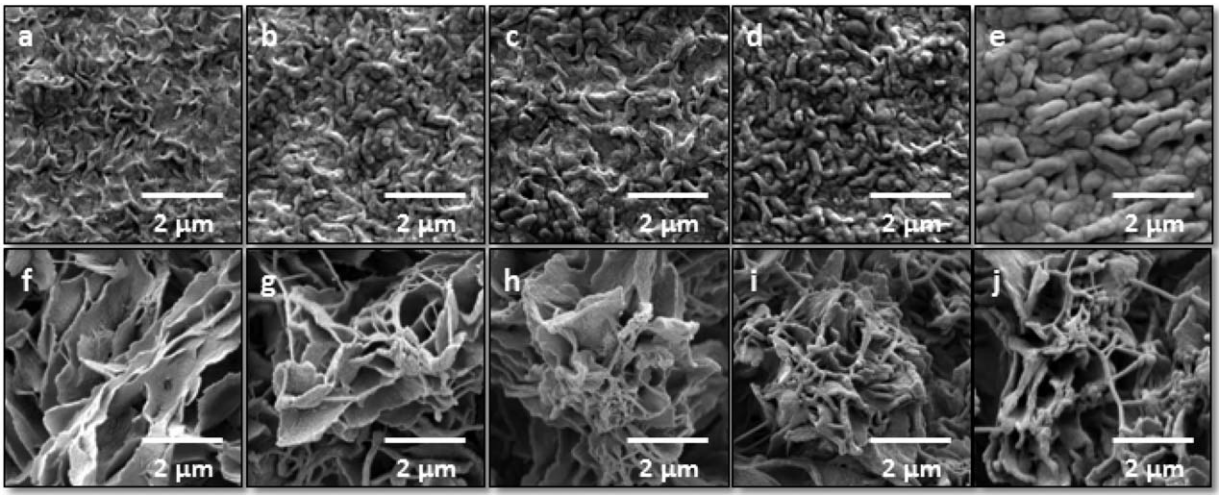

Figure 1. FESEM images of neat and ZnO-embedded HDPE membranes. Upper surfaces: (a) neat HDPE, (b) 0.25 wt % ZnO, (c) 0.50 wt % ZnO, (d) 0.75 wt % ZnO, (e) 1.0 wt % ZnO. Cross-sections: (f) neat HDPE, (g) 0.25 wt % ZnO, (h) 0.50 wt % ZnO, (i) 0.75 wt % ZnO, (j) 1.00 wt % ZnO.

$$J_r = \frac{J}{J_n} \tag{3}$$

where J_n is the PWF of neat PE membrane. Each sample was tested 3 times and average values of PWF were used to calculate the relative PWF and used for further analysis.

Performance of Membranes

The performance of neat and ZnO-embedded membranes was evaluated by filtration of humic acid solution as an important water contaminant. The solution was prepared by dissolving 1 g of humic acid in 1 L of pure water. The solution was stirred during filtration and all the filtration experiments were conducted at trans-membrane pressure of 1.4 bar. The concentration of humic acid in the permeate was determined spectrophotometrically and the rejection of the humic acid was calculated as follows:

$$\mathrm{R}\ (\%) = \left(1 - \frac{\mathrm{C_p}}{\mathrm{C_f}}\right) \times 100 \tag{4}$$

where C_p and C_f are the permeate and feed concentrations of humic acid, respectively.

RESULTS AND DISCUSSION

SEM, EDX, and XRD

The SEM images of surface and cross-section of neat and ZnO-embedded HDPE membranes are shown in Figure 1. It can be seen that all membranes have leafy structures characterized by randomly oriented connected HDPE leaves. Generally, HDPE/mineral oil casting solutions with compositions in the range of 15–50 wt % HDPE undergo solid–liquid phase separation and, therefore, they are capable of producing membranes with leafy structures.[24]

Figure 1 shows that increasing the dosage of ZnO from 0 to 1 wt % increases the number of pores in the surface of membranes. This may be due to the heterogeneous nucleation effect of ZnO nanoparticles. When the casting solution of HDPE/MO/ZnO was quenched in water bath, ZnO nanoparticles acted as crystal nucleating agents,[17] and therefore, polymer chains were crystallized around the nuclei. As a result, clusters of ZnO-embedded HDPE were formed, resulting in finer pores in the surface and also the bulk of the membranes (see cross-section SEM images, Figure 1). On the other hand, the crystallization of polymer chains in HDPE/MO solution occurs somewhat differently so that heterogeneous nucleation does not exist and the HDPE lamellae, therefore, are formed more uniformly leading to lower density of the pores, in comparison to ZnO-embedded membranes.

The presence of ZnO nanoparticles in the membrane structure was confirmed by EDX analysis. The result of EDX analysis for neat and 1 wt % ZnO-embedded HDPE membranes is shown in Figure 2. The difference in the EDX spectra of the two membranes is clear confirming ZnO nanoparticles being present in the hybrid membrane. The same behavior was observed for 0.25, 0.50, and 0.75 wt % ZnO-embedded HDPE membranes (data are not shown).

The presence of ZnO nanoparticles was also confirmed by XRD analysis. XRD diffraction patterns of ZnO nanoparticles, HDPE, and 1 wt % ZnO-embedded HDPE membranes were presented in Figure 3. The XRD pattern of utilized ZnO nanoparticles showed four crystalline characteristic peaks at 2θ of 31.9°, 34.6°, 36.5°, and 56.8°which is in agreement with the literature.[21] Two sharp peaks at 2θ of 21.6° and 24° are characteristic peaks of HDPE.[25] The diffraction curve of ZnO-embedded HDPE membrane showed the peaks at 2θ of 21.6°, 24°, 31.9°, 34.6°, and 36.5° indicating that ZnO nanoparticles have been distributed to the membrane matrix. It also shows that the addition of nanoparticles did not affect the crystalline phase of ZnO-embedded HDPE membrane. The same results were observed for 0.25, 0.50, and 0.75 wt % ZnO-embedded HDPE membranes and are not shown here.

Differential Scanning Calorimetry

DSC is one of the most important techniques of thermal analysis for studying the crystallization characteristics of polymeric

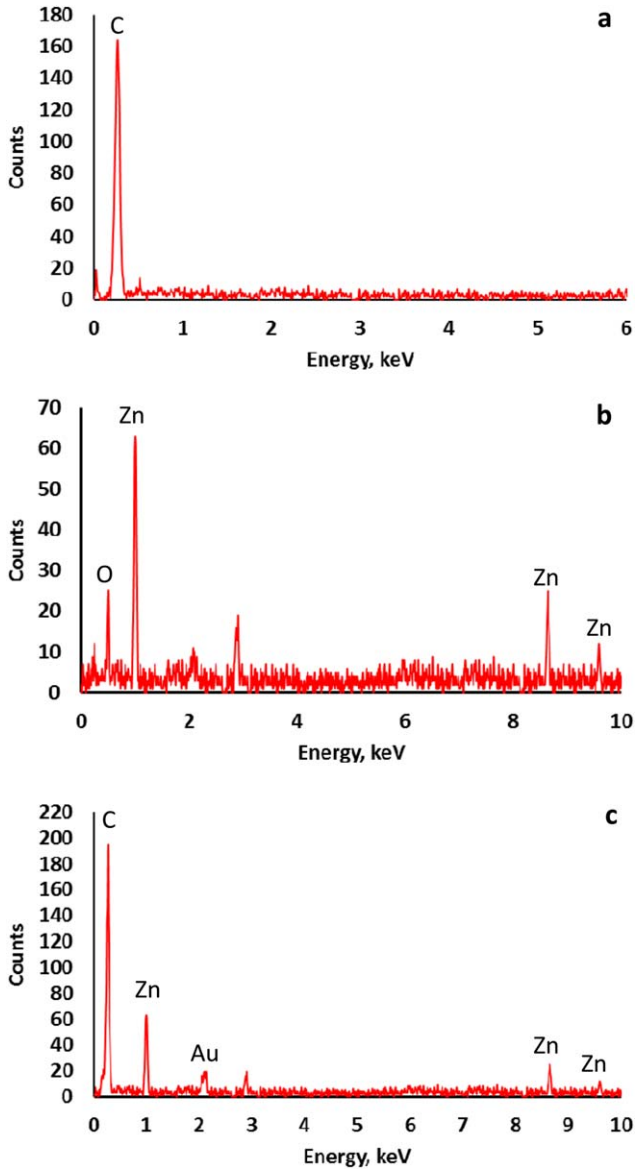

Figure 2. EDX results of (a) neat, (b) ZnO nanoparticles, and (c) 1.00 wt % ZnO-embedded HDPE membranes. [Color figure can be viewed in the online issue, which is available at wileyonlinelibrary.com.]

Table I. Differential Scanning Calorimetric Analysis of Neat and ZnO-Embedded HDPE Membranes

ZnO content (wt %)	T_m (°C)	T_c (°C)	$\Delta H_m(J/g)$	χ_c(%)
0.00	127.50	110.14	159.19	54.33
0.25	128.04	110.71	159.98	55.17
0.50	128.61	109.92	161.31	56.23
0.75	128.97	110.38	162.72	57.35
1.00	129.42	109.54	163.84	58.36

materials and composites. DSC data for neat and ZnO-embedded membranes including melting point, crystallization temperature, heat of melting, and percentage of crystallinity are summarized in Table I. Furthermore, the second heating scans of the samples are depicted in Figure 4. From Table I, it can be seen that the crystallinity of the membranes increased by increasing ZnO content. The melting behavior of the membranes, as reflected by both ΔH_m and T_m, was also increased by increasing ZnO content even though the crystallization temperature was not affected.

The increase in crystallinity of membranes indicates that ZnO particles act as nucleating agents during quenching of the casting solution and facilitate crystallization of HDPE resulting in higher crystallinity. It is generally accepted that nanoparticles act as nucleating agents in polymer crystallization.[26] However, different results have been obtained from other experimental observations. For example, Chan *et al.* reported that incorporation of $CaCO_3$ nanoparticles into polypropylene (PP) do not affect PP crystallinity.[27] In another work, the crystallinity of PP/ZnO composites has been reported to increase from 38.7% for PP to 41.1% for 5% ZnO/PP composite as reported by Zhao and coworkers.[26] Nguyen *et al.* have shown that the presence of TiO_2 nanoparticles decreases crystallinity of low-density polyethylene/TiO_2 nanocomposites.[28]

Thermogravimetric Analysis

To examine if ZnO nanoparticles are well dispersed in the membrane matrix, TGA was carried out on the neat and

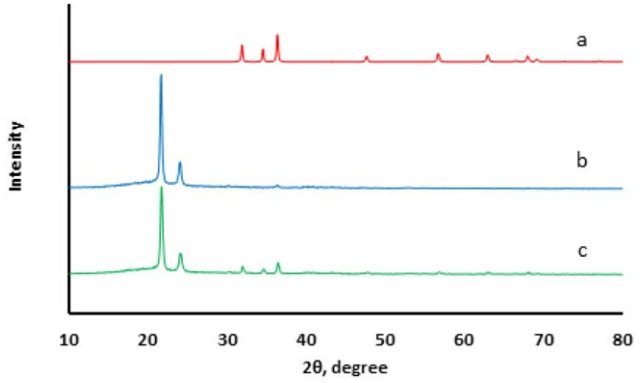

Figure 3. XRD patterns of (a) ZnO nanoparticles, (b) HDPE membrane, and (c) 1.00 wt % ZnO-embedded HDPE membrane. [Color figure can be viewed in the online issue, which is available at wileyonlinelibrary.com.]

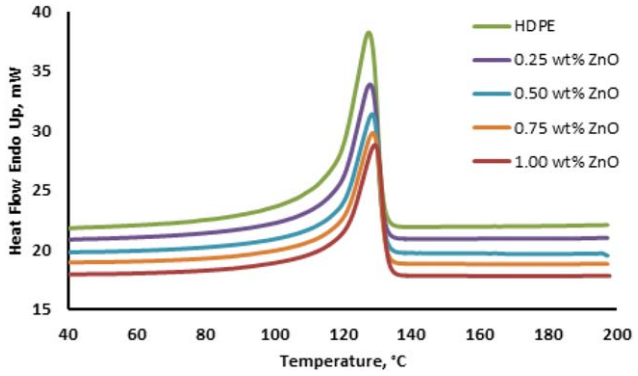

Figure 4. DSC second heating of neat and ZnO-embedded HDPE membranes. [Color figure can be viewed in the online issue, which is available at wileyonlinelibrary.com.]

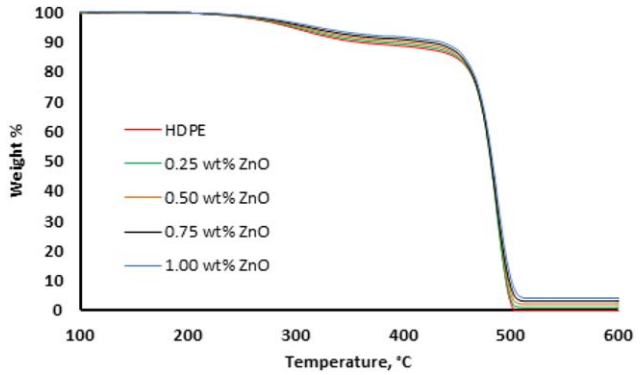

Figure 5. TGA thermograms of neat and ZnO-embedded HDPE membranes. [Color figure can be viewed in the online issue, which is available at wileyonlinelibrary.com.]

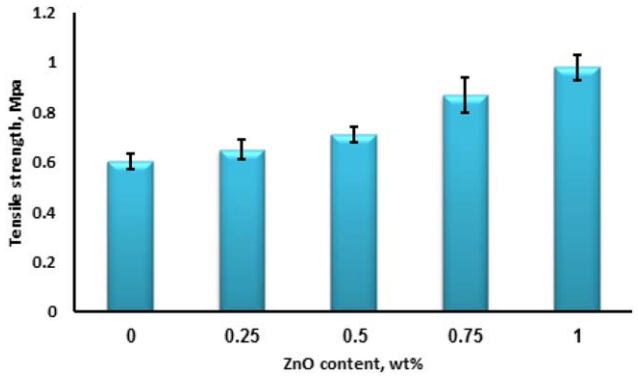

Figure 6. Tensile strength of neat and ZnO-embedded HDPE membranes. [Color figure can be viewed in the online issue, which is available at wileyonlinelibrary.com.]

ZnO-embedded HDPE membranes. For each membrane, three different pieces from different parts of a flat sheet membrane were cut and used. Figure 5 shows the results for neat and ZnO-embedded HDPE membranes. It can be seen that, for example, the residue for 1.00 wt % ZnO-embedded HDPE membrane is 4.18% which indicates that ZnO nanoparticles were well dispersed throughout the membrane. The casting solution of 1.00 wt % ZnO-embedded HDPE membrane contained 1.00 g ZnO, 20.00 g HDPE, and 79.00 g MO. Therefore, the final amount of ZnO in the membrane should be 4.76%, which is very close to the obtained result of 4.18%. It should be noticed that the presence of all amount of the particles in the final membrane is definitely impossible because some amounts of particles could leach out during membrane fabrication process. Therefore, the final amount of particles in the membrane is always lower than its theoretical value and the difference between these values is reasonable. Thus, the results confirm good dispersion of ZnO nanoparticles in the membrane as well as insignificant loss of nanoparticles during membrane fabrication process. The same set of experiments was conducted for 0.25, 0.50, and 0.75 wt % ZnO-embedded HDPE membranes and the results were summarized in Table II. The data in Table II show that the difference between expected and real amounts of particles in the membranes increased with decreasing ZnO content in the casting solution which indicates higher values of nanoparticles, e.g., more than 1.00 wt %, may be used in fabrication of these membranes.

Mechanical Behavior

Elongation and mechanical strength at break are two important parameters to describe the mechanical behavior of membranes.

Table II. Expected and Experimental Residual Values (wt %) for Different ZnO-Embedded HDPE Membranes

ZnO content (wt %)	Expected ZnO in membrane (wt %)	Residual from TGA (wt %)
0.25	1.24	1.04
0.50	2.44	2.09
0.75	3.61	3.16
1.00	4.76	4.18

These two parameters for the fabricated membranes are depicted in Figures 6 and 7. The addition of nanoparticles into polymer alters the mechanical properties of polymers.[28] It can be seen that the mechanical strength of the membranes has increased by increasing the content of ZnO nanoparticles in the casting solution while the elongation has decreased which is mainly due to the reinforcement effect of the inorganic nanoparticles. Wu *et al.* showed that dispersion of the TiO_2 nanoparticles in PES membranes act as physical cross-links to bear the stress of the load and, therefore, improve the membrane mechanical strength.[29] The same results were obtained by Cui *et al.* which prepared SiO_2/PVDF membranes via TIPS method. They observed that tensile strength of membranes increased as the content of SiO_2 increased from 0 to 2 wt % and then decreased at higher contents.[19]

More information about mechanical characteristics of membranes can be obtained by DMA. Figure 8 shows the storage modulus of neat and ZnO-embedded HDPE membranes. There is a decreasing trend of the storage modulus (E') values for all the membranes with increase in temperature. Moreover, it can be observed that the storage modulus has increased with increasing ZnO content in the membranes owing to the stiffness improvement effect of inorganic ZnO nanoparticles.[26] Generally, storage modulus decreases with temperature due to the

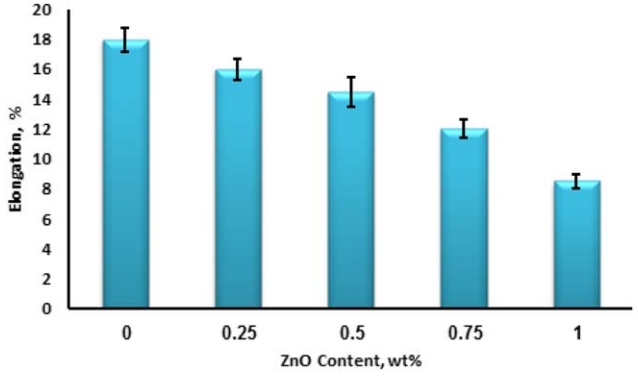

Figure 7. Elongation at break of neat and ZnO-embedded HDPE membranes. [Color figure can be viewed in the online issue, which is available at wileyonlinelibrary.com.]

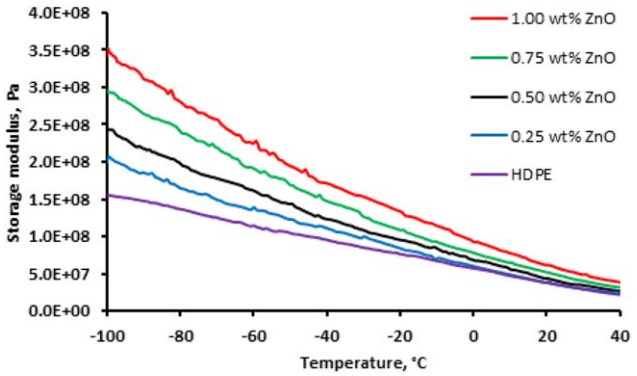

Figure 8. Storage modulus *vs* temperature plots for neat and ZnO-embedded HDPE membranes. [Color figure can be viewed in the online issue, which is available at wileyonlinelibrary.com.]

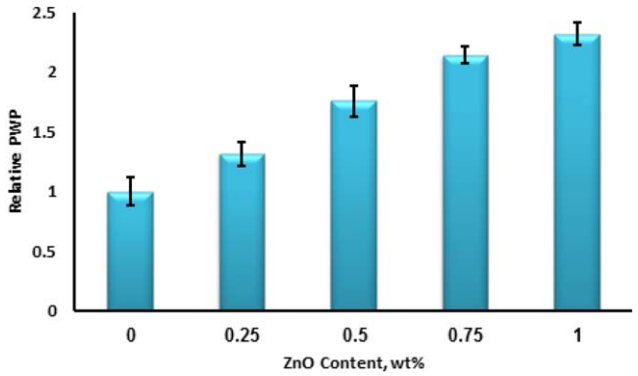

Figure 10. Relative pure water flux of neat and ZnO-embedded HDPE membranes. [Color figure can be viewed in the online issue, which is available at wileyonlinelibrary.com.]

increased thermal motions of the side chains and agitation in the interspatial region between the amorphous and crystalline regions.[30] However, addition of inorganic nanoparticles may hinder these movements, so that at any temperature, E' values increase with ZnO content.

The variations of loss modulus (E'') with temperature for the membranes are shown in Figure 9. In DMA, the E″ indicates the amount of energy which dissipates as heat due to the internal friction between polymer chains. From Figure 9, it can be seen that at any temperature, loss modulus increased with increasing the content of ZnO nanoparticles. For neat and composite HDPE membranes, there are two main peaks. The first loss peak in the temperature range of −80 to −70°C is related to glass transition temperature of HDPE.[31] The second peak in the range of 0 to 20°C is related to α-transition region of HDPE.[30,32,33] As can be seen from Figure 8, the addition of ZnO particles does not have any obvious effect on the glass transition temperature of membranes which may be due to the low content of ZnO particles.

Pure Water Flux

The effect of ZnO nanoparticles on PWF of membranes is shown in Figure 10. The data in Figure 10 are relative PWF which is defined as the PWF of membranes divided by PWF of neat HDPE membrane. Generally, it can be seen that the addition of ZnO nanoparticles in the casting solution has increased PWF of membranes. The increase in the PWF is related to the number of pores in the membrane surface as well as the increase in membranes hydrophilicity. As mentioned earlier, increasing the dosage of ZnO from 0 to 1 wt % increased the number of pores in the surface of membranes due to the heterogeneous nucleation effect of ZnO nanoparticles. Therefore, more number of pores leads to higher water flux of membranes. Moreover, it has been shown that the contact angle of the membranes decreased from 118° for neat HDPE membranes to 110° for 1 wt % ZnO-embedded membrane which shows that the hydrophilicity of membranes increases with increasing the content of ZnO nanoparticles.[22] As a result, PWF of the membranes increased as the content of ZnO increased.

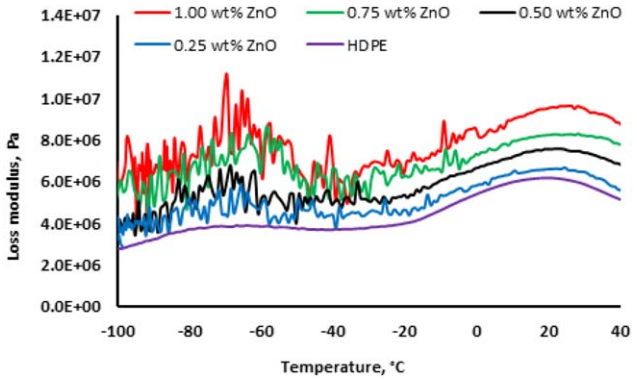

Figure 9. Loss modulus *vs* temperature plots for neat and ZnO-embedded HDPE membranes. [Color figure can be viewed in the online issue, which is available at wileyonlinelibrary.com.]

Performance of Membranes

The results of filtration of 1 g/L humic acid solution were summarized in Table III. It can be seen that pure HDPE membrane has the highest rejection value (60.3%) and with increasing the ZnO content in the membranes, rejection of the humic acid is decreased. The trend of rejection data is inconsistent with the mean pore radius of membranes[22] indicating that the rejection of membranes decreases with increasing mean pore radius. The results show that even though incorporation of nanoparticles improved thermal and mechanical properties of membranes, the performance of them decreased due to the increase in mean pore radius.

CONCLUSION

ZnO-embedded HDPE membranes were fabricated via TIPS method and characterized by a set of analyses. The results of

Table III. Rejection Performance of Neat and ZnO-Embedded HDPE Membranes in Separation of Humic Acid Solution

ZnO content wt %	Rejection (%)
0.00	60.3 ± 2.1
0.25	57.1 ± 2.0
0.50	53.9 ± 1.3
0.75	50.4 ± 2.7
1.00	47.2 ± 1.00

FE-SEM, EDX, XRD, and TGA analyses confirmed the presence of ZnO nanoparticles in the polymer matrix. The results of DSC analysis revealed that the melting points as well as the crystallinity of the membranes increase slightly with increasing ZnO content. Addition of nanoparticles also increased storage modulus, loss modulus, and tensile at break of the membranes due to the stiffness improvement effect of inorganic ZnO. However, glass transition temperature of the membranes was not affected by presence of particles. Incorporation of nanoparticles improved PWF of the membrane due to the increase of the number of pores on the surface of membranes as well as increase of hydrophilicity.

REFERENCES

1. Ulbricht, M. *Polymer* **2006**, *47*, 2217.
2. Jafarzadeh, Y.; Yegani, R. *Chem. Eng. Res. Des.* **2015**, *93*, 684.
3. Liang, S.; Xiao, K.; Mo, Y.; Huang, X. *J. Membr. Sci.* **2012**, 394, *184*.
4. Balta, S.; Sotto, A.; Luis, P.; Benea, L.; Van der Bruggen, B.; Kim, J. *J. Membr. Sci.* **2012**, *389*, 155.
5. Rahimpour, A.; Madaeni, S. S.; Taheri, A. H.; Mansourpanah, Y. *J. Membr. Sci.* **2008**, *313*, 158.
6. Ulbricht, M.; Belfort, G. *J. Membr. Sci.* **1996**, *111*, 193.
7. De Sitter, K.; Dotremont, C.; Genne, I.; Stoops, L. *J. Membr. Sci.* **2014**, *471*, 168.
8. Vatanpour, V.; Madaeni, S. S.; Khataee, A. R.; Salehi, E.; Zinadini, S.; Monfared, H. A. *Desalination* **2012**, *292*, 19.
9. Xi, Z.-y.; Xu, Y.-Y.; Zhu, L.-P.; Du, C.-H.; Zhu, B.-k. *Polym. Adv. Technol.* **2008**, *19*, 1616.
10. Zhang, C.; Bai, Y.; Sun, Y.; Gu, J.; Xu, Y. *J. Membr. Sci.* **2010**, *365*, 216.
11. Kolesov, I. S.; Kratz, K.; Lendlein, A.; Radusch, H.-J. *Polymer* **2009**, *50*, 5490.
12. Mosadegh-Sedghi, S.; Rodrigue, D.; Brisson, J.; Iliuta, M. C. *Polym. Adv. Technol.* **2013**, *24*, 584.
13. Liu, J.-H.; Jen, H.-L.; Chung, Y.-C. *J. Appl. Polym. Sci.* **1999**, *74*, 2947.
14. Zhang, J.; Jiang, D. D.; Wilkie, C. A. *Polym. Degrad. Stab.* **2006**, *91*, 641.
15. Zhang, J.; Jiang, D. D.; Wilkie, C. A. *Thermochim. Acta* **2005**, *430*, 107.
16. Bottino, A.; Capannelli, G.; Comite, A. *Desalination* **2002**, *146*, 35.
17. Shi, F.; Ma, Y.; Ma, J.; Wang, P.; Sun, W. *J. Membr. Sci.* **2012**, *389*, 522.
18. Yan, L.; Li, Y. S.; Xiang, C. B. *Polymer* **2005**, *46*, 7701.
19. Cui, A.; Liu, Z.; Xiao, C.; Zhang, Y. *J. Membr. Sci.* **2010**, *360*, 259.
20. Leo, C. P.; Cathie Lee, W. P.; Ahmad, A. L.; Mohammad, A. W. *Sep. Purif. Technol.* **2012**, *89*, 51.
21. Shen, L.; Bian, X.; Lu, X.; Shi, L.; Liu, Z.; Chen, L.; Hou, Z.; Fan, K. *Desalination* **2012**, *293*, 21.
22. Jafarzadeh, Y.; Yegani, R.; Sedaghat, M. *Chem. Eng. Res. Des.* **2015**, *94*, 417.
23. Wunderlich, B. Thermal Analysis; Academic Press: New York, **1990**, p 417.
24. Lloyd, D. R.; Kinzer, K. E.; Tseng, H. S. *J. Membr. Sci.* **1990**, *52*, 239.
25. Han, G.; Lei, Y.; Wu, Q.; Kojima, Y.; Suzuki, S. *J. Polym. Environ.* **2008**, *16*, 123.
26. Zhao, H.; Li, R. K. Y. *Polymer* **2006**, *47*, 3207.
27. Chan, C.-M.; Wu, J.; Li, J.-X.; Cheung, Y.-K. *Polymer* **2002**, *43*, 2981.
28. Nguyen, V. G.; Thai, H.; Mai, D. H.; Tran, H. T.; Tran, D. L.; Vu, M. T. *Compos. Part B: Eng.* **2013**, *45*, 1192.
29. Wu, G.; Gan, S.; Cui, L.; Xu, Y. *Appl. Surf. Sci.* **2008**, *254*, 7080.
30. Sewda, S.; Maiti, S. N. *Polym. Bull.* **2013**, *70*, 2657.
31. Brandrup, J.; Immergut, E. H.; Grulke, E. A. Polymer Handbook; Wiley: New York, **1999**, Part V, Chapter 7, p 234.
32. Sirotkin, R. O.; Brooks, N. W. *Polymer* **2001**, *42*, 9801.
33. Khonakdar, H. A.; Morshedian, J.; Wagenknecht, U.; Jafari, S. H. *Polymer* **2003**, *44*, 4301.